

Translocation Properties of Polymer Chains Through Pore Based on Computer Simulation

1 Introduction

Polymer translocation through channels/pores from one side to the other side frequently occurs in microbiology activities. For example, proteins thread through the channels on cytomembrane to support chemical reactions in organisms. For the past few decades, polymer translocation properties become significant and popular research topics as algorithm and discussion of computer simulation for enormous amount of calculation like polymer chains Mento Carlo simulation or molecular dynamics have become mature. Theoretically speaking, the process of threading involves the transportation of a polymer from a free-apace region, where many conformations are allowed, through a narrow hole where the number of allowed conformations is drastically reduced. Consequently the chains transport across an entropic barrier. Among all Mento Carlo simulations of polymer chains and theoretical researches of translocation, required translocation time and possibility for the chain to fully thread through and their correlation with polymer properties like lengths and bending rigidity are most investigated topics. In application, polymer translocation, which reflects different phenomenons as individual monomers threading through, can be determined as the core of future DNA sequencing technology.

2 Experiments in polymer translocation

As Kasianowicz's work on DNA/RNA translocation through 2.6 nm diameter ion channel in a lipid bilayer membrane [1] concluded, due to the fact that only one single-stranded polymer can thread through the channel at certain time, the channel is partially or totally blocked during the translocation process. Moreover, we usually take electric field as driven force for polymers, which usually result in electric currents across the channel,

to accelerate the translocation process and increase successful possibility as non-driven translocation takes considerable time and resources to observe and record the entire process due to the stochastic Brownian motion. Thus, as soon as the translocation process begins, there should be noticeable current drop (experimentally speaking, the drops are large as 85-100%), which makes it possible to use the blockage as a method to determine the length of polymers (we now assume that the longer polymers are, the more time they need to completely translocate, which can be confirmed later with experiment data). What's more, once we are able to discovery the reflection of individual monomers threading through channel, we find a way to determine the exact sequence of polymers.

In experiment, Kaianowicz use α -hemolysin to form a single channel across a lipid bilayer separating two buffer-filled compartments and poly[A], poly[U], poly[C] along with other polyuridylic acids are chosen to thread through the channel under electric field.

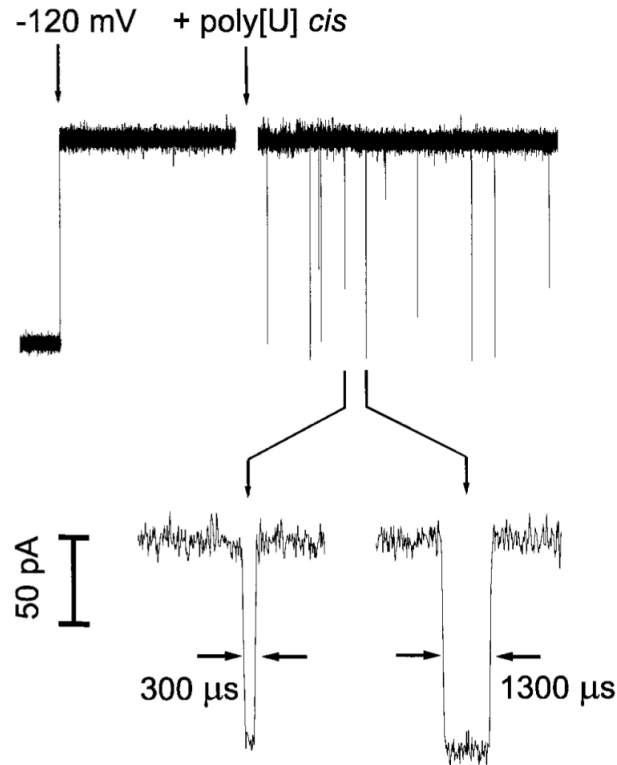


Figure 1: The current drop while translocation process begins

As we noticed the tracked current drop in Figure.1, once the 120 mV electric field turns on and we put poly[U] on *cis* side, the translocation process

begins, which results in the blockages and current drops. The current drops are noticeably large at about 85-100% and for each polymer, the blockage time is probably different due to their individual lengths and driving forces.

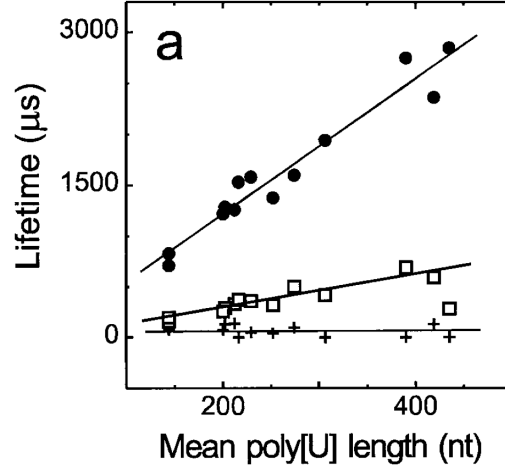


Figure 2: The blockade lifetimes' dependence of polymer lengths

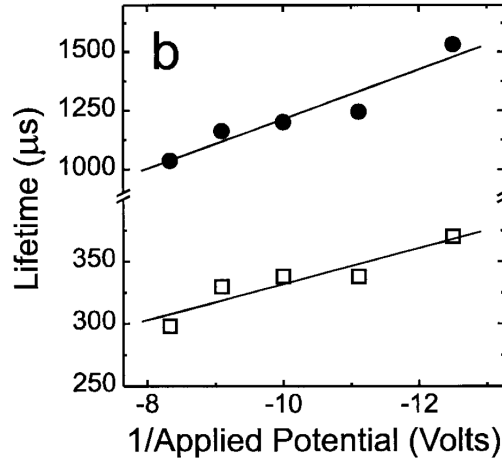


Figure 3: The blockade lifetimes' dependence of electric field

By plotting the dependence of blockade lifetimes over polymer lengths (shown in Figure.2) and electric field (shown in Figure.3), we find that the lifetimes are proportional to polymer lengths and inversely proportional to electric field, which can be explained by physical sense that the longer polymers

are, the more time they need to complete the translocation process, and the higher electric fields are, the stronger driven forces are, which result in the shorter time polymer required.

Moreover, using single-molecule methods, we are able to determine the effect of Ions on modifying the structure and mechanical properties of DNA, which turns out to be [2] : (i) The electrostatic contribution to persistence length P varies as the inverse of the ionic strength I ; (ii) Ions in which the charge is centrally concentrated lead to lower P values; (iii) The elastic stretch modulus and persistence length display opposite trends with ionic strength; (iv) DNA is still well described by the WLC model at concentrations of trivalent cations capable of inducing dNA collapse or condensation; (v) Buckling transition that has been postulated to underlie condensation haven't been observed.

3 Theoretical work in polymer translocation and melt

3.1 Properties of polymer melt

Two of the most widely used theories for polymer melt dynamics reduce the problem to a single chain motion in an effective medium: the *Rouse model* for the simple case of unentangled chains and the *reptation model* for entangled chains. According to the *Rouse model*, a Gaussian chain of beads connected by springs interacts with a stochastic medium that mimics the presence of the other chains, which results in the consequence that the self-diffusion coefficient D scales with the chain length N as $N \propto N^{-1}$. While in *reptation model*, the polymer chain is confined inside a "tube" formed by the constraints imposed by the entanglements with other chains, and the self-diffusion coefficient scales as N^{-2} . [3]

Considering the static and dynamic properties of polymer chains in a melt: [4] For fully equilibrated large polymer melts, we observe that for moderately stiff chain ($k_\theta = 1.5$), the ratio $\langle R_e^2 \rangle / \langle R_g^2 \rangle \approx 6$ as expected for ideal chains. For fully flexible chains ($k_\theta = 0$), results of the mean square internal distance $\langle R^2(s) \rangle$ show remarkable deviations from the freely rotating chain model describing the behavior of ideal chains, while the deviations are diminished as the stiffness of chains increases. For $k_\theta = 1.5$, $\langle R^2(s) \rangle$ is in perfect agreement with FRC (freely rotating chain) model up to $N \approx 800$, while a slight deviation occurs for $N > 800$ due to the correlation hole effect. Results of the probability distribution of reduced end-to-end distance $r_e = (R_e^2 / \langle R_e^2 \rangle)^{1/2}$ and reduced gyration radius $r_g = (R_g^2 / \langle R_g^2 \rangle)^{1/2}$ for

polymer chains in a melt for various values of N and for $k_\theta = 1.5$ show the nice data collapse and are described by universal functions for ideal chains.

Moreover, by investigating the properties of fully equilibrated polymer chains in a melt, we find that the coarse-grained bead-spring model is an ideal model. It marks a good compromise between chain flexibility and small entanglement length. While the flexibility allows for relatively large time steps and the application of recently developed equilibration schemes, the moderate stiffness warrants small deviations from ideality and at the same time relatively small entanglement lengths, which are decisive for comparably small, though still huge, relaxation times. Therefore, we expect that this model can serve as an optimal test case, where one can gain insight into non-linear viscoelasticity regime for large polymer melts by non-equilibrium molecular dynamics simulations.

3.2 Properties of polymer translocation

In driven translocation, entropic barrier becomes negligible and the translocation time depends mainly on the applied field. An important measure is the scaling of translocation time with polymer length N and force intensity f , $\tau \propto N^\alpha f^{-\delta}$, where both α and δ are constants that vary with different situations. [5]

The continuity equation for $P(s,t)$, the probability of finding segment s in the pore at time t , can now be rewritten as:

$$\frac{\partial P(s,t)}{\partial t} = (-v \frac{\partial}{\partial s} + D \frac{\partial^2}{\partial s^2}) P(s,t) \quad (3.1)$$

The equation leads to an exponential first passage time distribution, $Q(t) \propto \exp[-\frac{(L-vt)^2}{4Dt}]$ as expected for a Brownian process. The mean translocation time scales as $\tau \propto N^\alpha f^{-\delta}$ with $\alpha = 1$ and $\delta = 1$.

The threading polymer encounters a chemical potential difference $\Delta\mu \equiv (\mu_+ - \mu_-) > 0$ which provides the leading contribution to the free energy $F(s) = s\mu_+ + (N-s)\mu_-$. There exist two distinct regimes: (i) for a weak force, $f \propto N\Delta\mu/a \ll 1$, where the entropic barrier dominates the translocation process and $\tau \propto N^2$; (ii) the regime of a strong driving force, $N\Delta\mu/a > 1$, when $\tau \propto Nf^{-1}$.

The translocation process can be considered with Fokker-Planck equation:

$$\frac{\partial}{\partial t} p(m,t) = L_{FP}(m)(m,t) \quad (3.2)$$

where $p(m,t)$ is the possibility that there are m monomers in *trans* space at time t . And $L_{FP}(m)$ reads:

$$L_{FP}(m) = \frac{1}{l_0^2} \frac{\partial}{\partial m} D(m) e^{-\beta F(m)} \frac{\partial}{\partial m} e^{\beta F(m)} \quad (3.3)$$

In most of theoretical work, $D(m)$ is considered as constant D . While we define that m monomers in *trans* space, $N-m$ monomers are still in *cis* space. If the internal interaction along the polymer can be ignored, free energy $F(m)$ reads:

$$\beta F(m) = \begin{cases} (1 - \gamma) \ln[m(N - m)] + m\Delta\mu & , 0 < m < N \\ m\Delta\mu & , m = 0 \text{ or } N \end{cases} \quad (3.4)$$

Now the translocation time from *cis* side to *trans* side reads [6]:

$$\tau = \frac{\Psi(0, m_0) \Phi_+(m_0, N) - \Phi_+(0, m_0) \Psi(m_0, N)}{\Psi(0, m_0) \Psi(0, N)} \quad (3.5)$$

where [7]

$$\Psi(x, y) = \int_x^y dz \frac{1}{\phi(z)} \quad (3.6)$$

$$\Psi_+(x, y) = \int_x^y dp \frac{1}{\phi(p)} \int_0^p dq \frac{\phi(q) \Psi(0, q)}{D(q)} \quad (3.7)$$

$$\phi(y) = \exp\left[-\frac{1}{k_B T} \int_0^y dx \frac{\partial F_x}{\partial x}\right] \quad (3.8)$$

3.3 TP translocation theory

A break-through [8] in the problem of translocation process is the employment of tension propagation (TP) to explain the mechanism of this process. According to TP theory (shown in Figure.4), when the external driving force (usually caused by external electric field) acts on the beads at the pore in the direction of *cis* to *trans* side, a tension front propagates along the backbone of the chain in the *cis* side of the chain. Now we consider the *cis* side as mobile and immobile parts, where mobile part has been influenced by external force and tended to move towards the pore while the immobile part still stays in equilibrium state, i.e. its average velocity is zero.

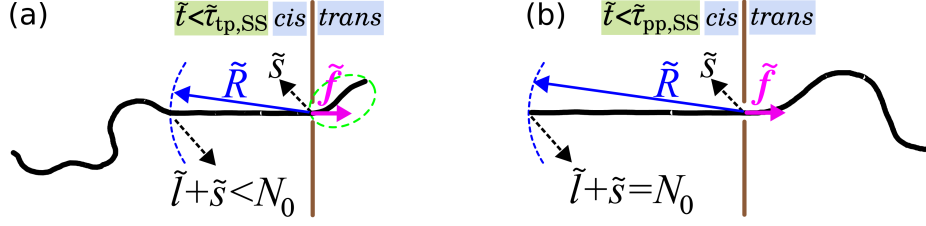


Figure 4: (a) A schematic of the translocation process in the tension propagation (TP) stage; (b) The translocation process for SS regime during the post propagation stage where the tension front has reached the chain end.

Following TP theory, due to the solvent during the course of translocation, Brownian dynamics - TP theory (BDTP) to take into account the effect of pore friction, finite chain length, and thermal fluctuations develops. More recently, the BDTP theory was reformulated within the constant monomer *iso-flux* approximation (IFTP), leading to a fully quantitative and self-consistent theory with only one free parameter, the effective pore friction.

In translocation dynamics, average translocation time is a function of the chain length as $\tau \approx N_0^\alpha$ ($\alpha = \nu + 1$). As for flexible chain, $\tau = a_p N_0 + a_c N_0^{\nu+1}$, where both a_p and a_c are constants. The first term is due to the pore friction which causes a significant finite-size correction to the asymptotic scaling. On the other hand, in the limit of a rod-like polymer $\tau \propto N_0^2$.

4 One intriguing example: Translocation of Diblock Copolymer through Compound Channel

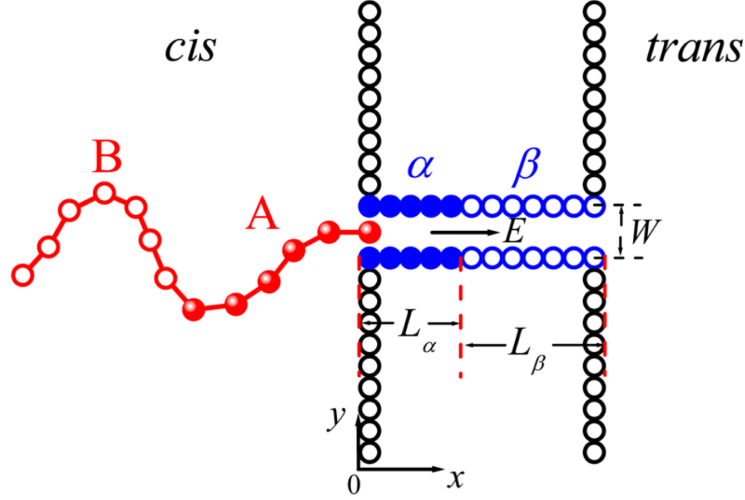


Figure 5: A stretch of copolymer threading through a compound channel

The particular model [9] focus on the translocation of diblock copolymer through compound channel. As seen in Figure.5, the copolymer is consist of two parts $A_{N_A}B_{N_B}$ and the compound channel is composed of part α with length L_α and part β with length L_β . To allow the copolymer to thread through the channel quickly, we set the interaction between polymer part A and channel part α as attractive while all other interactions should be considered as repulsive. All interaction parameters should be properly set to prevent the polymer move back to *cis* space or the attraction is so strong that polymer is unable to leave the channel.

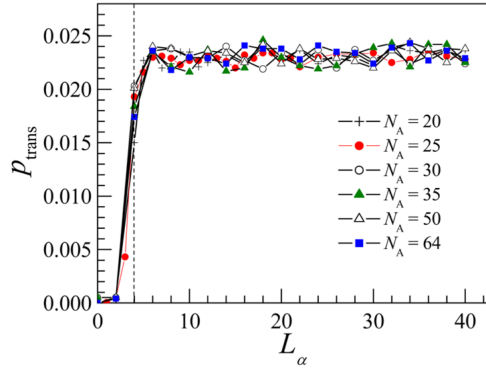


Figure 6: Translocation probability p_{trans} as a function of L_α for different N_{AS} .

Simulation about the dependence of translocation probability p_{trans} against L_α for different N_A shows in Figure.6: p_{trans} is about zero when $L_\alpha < 4$, and jumps quickly to a saturation value. The translocation probability increases with the increase in attraction strength and driving force.

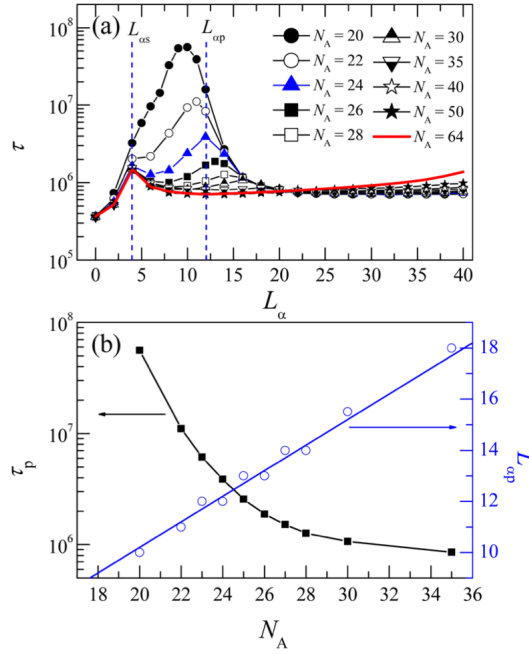


Figure 7: (a) Dependence of the translocation time τ on L_α for different N_{AS} ; (b) Dependence of τ_p and $L_{\alpha p}$ on N_A at moderate N_A regions.

Simulation about the dependence of translocation time τ against L_α for different N_A shows in Figure.7: For large N_{AS} , there is a small peak, which is named as satellite peak, at small L_α . And the value of satellite peak τ_s and its place $L_{\alpha s}$ are roughly independent of N_A . For appropriate N_{AS} , a second peak, principle peak, appears. However, value of principle peak τ_p and its place $L_{\alpha p}$ are dependent of N_A . τ_p decreases quickly as N_A increases, and $L_{\alpha p}$ increases linearly as N_A increases at about $L_{\alpha p} \approx 0.5N_A$. As $\tau_p \gg \tau_s$ at small N_A , the satellite peak is covered gradually by principle peak. Moreover, for satellite peak, τ_s increases with the decrease in E or increase in ϵ_{AN} , and $L_{\alpha s}$ increases with decrease in E or ϵ_{AN} . For principle peak, $L_{\alpha p}$ is independent of E and $\epsilon_{A\alpha}$, and τ_p increases with $\epsilon_{A\alpha}$ but decreases with E . However, the principle peak vanishes with increase in E or decrease in $\epsilon_{A\alpha}$.

The simulation tells that the translocation process is significantly influenced by L_α , and there are two maxima in translocation time at $L_{\alpha s}$ and $L_{\alpha p} = N_A b_x$.

5 Polymer Model

For DNA, it is known that both thermal fluctuations and equilibrium intrinsic bends contribute to the measurable persistence length, a . In general, both of these contributions are sequence dependent, which greatly complicates the problem. However, under the assumption that contribution of intrinsic curvature to DNA bending is negligibly small, which can be confirmed true, the measured value of a for a DNA fragment and its average bending rigidity are linearly correlated by Boltzmann factor, kT . [10]

The typical ideal chain model, the Gaussian chain, only takes into account short range elastic interactions which occur between neighboring monomers along the chain. However, a real chain has excluded volume interaction which is important for real polymer chains in good solvents, and a real chain is subject to bond bending, rotational and torsional angles constraints, therefore has local rigidity. In simulations, FENE potential is frequently used. For modeling a polymer chain with excluded volume interaction and chain stiffness, we introduce Weeks-Chander-Anderson (WCA) potential, bending potential and FENE potential to model excluded volume interaction, chain stiffness and chain connection respectively. [11]

(i) The interaction between bonded beads use FENE potential:

$$U_{FENE}(b) = \begin{cases} -\frac{k_F}{2}(b_{max} - b_{eq})^2 \ln[1 - (\frac{b - b_{eq}}{b_{max} - b_{eq}})^2] & , b_{min} < b < b_{max} \\ \infty & , otherwise \end{cases} \quad (5.1)$$

where in the simulation, elastic coefficient $k_F = 300$, b is bond length, with bond length constraints: maximum bond length $b_{max} = 1.3$, minimum bond length $b_{min} = 0.3$, equilibrium bond length $b_{eq} = 0.8$ (under the constraint $2b_{eq} = b_{max} + b_{min}$).

(ii) The bending potential reads:

$$U_{bend}(\theta) = \frac{1}{2}k_\theta(\theta - \theta_0)^2 \quad (5.2)$$

where bending modulus k_θ represents the stiffness, θ is the angle between neighboring monomers. While $k_\theta > 0$, the stiffness appears and when $k_\theta \rightarrow \infty$, the bond-spring model becomes a rodlike chain model.

(iii) The interactions between nonbonded monomers with distance r in polymer using LJ potential:

$$U_{LJ}(r) = \begin{cases} 4\epsilon[(\frac{\sigma}{r})^{12} - (\frac{\sigma}{r})^6] - 4\epsilon[(\frac{\sigma}{r_{cut}})^{12} - (\frac{\sigma}{r_{cut}})^6] & , r < r_{cut} \\ 0 & , r \geq r_{cut} \end{cases} \quad (5.3)$$

where ϵ is the interaction intensity, σ is the diameter of monomers, r is the distance between monomers and cut-off distance $r_{cut} = 2^{1/6}$.

(iv) The interaction between bonds and walls uses WCA potential:

$$U_{WCA}(r) = \begin{cases} 4\epsilon_{PW}[(\frac{\sigma}{r})^{12} - (\frac{\sigma}{r})^6 + \frac{1}{4}] & , r < 2^{1/6}\sigma \\ 0 & , r \geq 2^{1/6}\sigma \end{cases} \quad (5.4)$$

where WCA interaction intensity $\epsilon_{PW} = 1$ in the simulation, r is the distance between monomers and walls.

Additionally, we notice that the bead-spring model should satisfies three requirements to simulate the actual polymer chain: (i) excluded-volume for each monomers, apparently, one monomer can't overlap with another; (ii) bonds can't intersect with each other, as bonds can be seen as "molecules", the repulsive force drive them away from each other; (iii) the bond length maintains in a defined range as the combination of flexibility and rigidity.

6 Monte Carlo Simulation

6.1 Polymer Statistics

For polymer chain with $N+1$ monomers, define their number from 0 to N . The first monomer is fixed at origin, and other monomers' position vectors are defined as $\{\mathbf{R}\}$, bonded monomer vectors are defined as $\{\mathbf{r}\}$. Thus, $\mathbf{r}_j = \mathbf{R}_j - \mathbf{R}_{j-1}$.

Polymer Hamiltonian then is expressed as:

$$H(\{\mathbf{R}\}) = \sum_{j=1}^N u_j(\mathbf{R}_{j-1}, \mathbf{R}_j) + w(\{\mathbf{R}\}) \quad (6.1)$$

or

$$H(\{\mathbf{r}\}) = \sum_{j=1}^N u_j(\mathbf{r}_j) + w(\{\mathbf{r}\}) \quad (6.2)$$

where u_j is the bond energy of monomer j , and w is the combination of other potentials.

Then we are able to find all statistics of polymers.
The partition function reads:

$$Z = \sum_i \exp[-H\{\mathbf{r}_i\}/k_B T] \quad (6.3)$$

And the possibility for particular conformation \mathbf{r} reads:

$$P(\{\mathbf{r}\}) = \frac{1}{Z} \exp[-H(\{\mathbf{r}\})/k_B T] \quad (6.4)$$

And the statistical average of particular physical quantity expresses as:

$$\langle A(\{\mathbf{r}\}) \rangle = \frac{1}{Z} \int A(\{\mathbf{r}\}) \exp[-H(\{\mathbf{r}\})/k_B T] d\{\mathbf{r}\} \quad (6.5)$$

6.2 Monte Carlo Simple Sampling

Sampling method means to stochastically choose M conformations from space, $\mathbf{r}_1, \mathbf{r}_2, \dots, \mathbf{r}_M$, and calculate quantity average by

$$\langle A(\{\mathbf{r}\}) \rangle \approx \overline{A(\{\mathbf{r}\})} = \frac{\sum_{l=1}^M A(\{\mathbf{r}\}_l) \exp[-\frac{H(\{\mathbf{r}\}_l)}{k_B T}]}{\sum_{l=1}^M \exp[-\frac{H(\{\mathbf{r}\}_l)}{k_B T}]} \quad (6.6)$$

while $M \rightarrow \infty$, $\langle A(\{\mathbf{r}\}) \rangle = \overline{A(\{\mathbf{r}\})}$.

Due to the fact that **Mento** Carlo simple sampling ignores Boltzmann factor, it leads to easy access to conformation distribution under different temperatures, however, while the low-energy conformation contains significant Boltzmann factor, the low-energy or specifically the low-temperature conformation calculation using simple sampling disagree with real conformation distribution.

6.3 Dynamic Mento Carlo Method

This method considers the possibility of certain conformations which reads as:

$$P_{eq}(\{\mathbf{r}\}_l) \propto \frac{1}{Z} \exp[-\frac{H(\{\mathbf{r}\}_l)}{k_B T}] \quad (6.7)$$

One classical method is Metropolis algorithm. Considering two states i and j , with energy E_i and E_j respectively, thus, their possibility reads:

$$P_i \propto \exp(-E_i/k_B T) \quad (6.8)$$

$$P_j \propto \exp(-E_j/k_B T) \quad (6.9)$$

Define the possibility of transforming from state i to j as p_{ij} , conversely, p_{ji} for j to i . According to requirement of equilibrium state, detail condition should be satisfied:

$$P_i p_{ij} = P_j p_{ji} \quad (6.10)$$

Now, if $p_{ji} = 1$,

$$p_{ij} = \exp[-(E_j - E_i)/k_B T] \quad (6.11)$$

Thus, in those conditions, statistical average reads:

$$\langle A \rangle \approx \bar{A} = \frac{\sum_{l=1}^M A \exp[-\frac{H(\{\mathbf{r}\}_l)}{k_B T}]/P(\{\mathbf{r}\}_l)}{\sum_{l=1}^M \exp[-\frac{H(\{\mathbf{r}\}_l)}{k_B T}]/P(\{\mathbf{r}\}_l)} \quad (6.12)$$

7 Dynamic Mento Carlo Simulation of Translocation Process

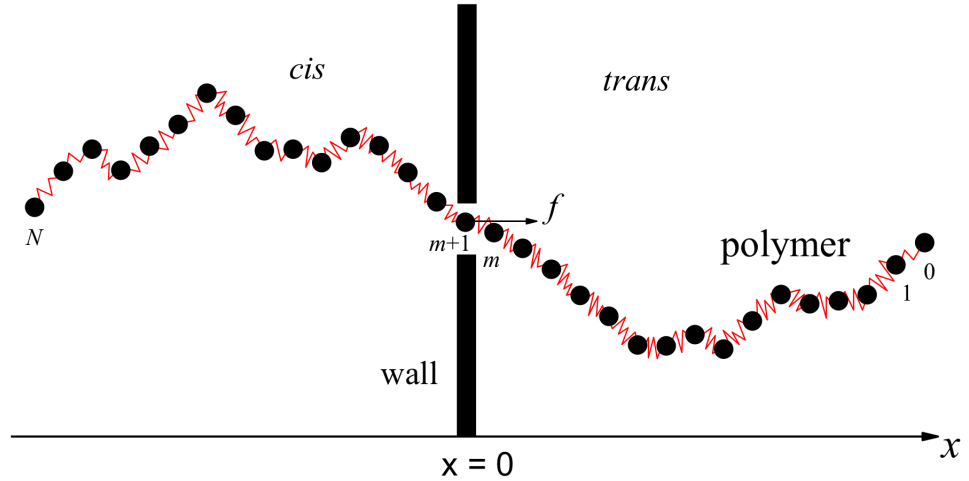


Figure 8: A 2D sample of semi-flexible polymer chain translocating from *cis* side to *trans* side

The simulated system of polymer chain and wall shows in Figure.8. The whole space is divided into two parts: *cis* ($x < 0$) and *trans* ($x > 0$) by a invincibly hard wall at $x=0$ with a pore on it. Before the translocation begins, the polymer is initially placed in *cis* space at equilibrium state and the pore is under the pressure of electric field, polymer tries to thread through the pore on the wall and transport into *trans* space.

The polymer generation: initially, the first monomer is fixed at the pore which is now closed in case the polymer partially cross the boundary, and then randomly generate monomers in *cis* space one by one under constraints required. The constraints mentioned here include: (i) volume being excluded; (ii) bonds never crossed; (iii) bonds length within resilience. And the system reaches equilibrium state before translocation begins. Then the polymer moves to equilibrium state to an unfolded condition for shorter translocation and simulation time.

Now the pore is open and the translocation begins while the time is set as $t = 0$. Randomly choose one monomer along the polymer chain and the chosen monomer randomly move in the space. However, some trial moves perhaps break the constraints mentioned above which are not allowed in polymer dynamics. In those cases, the system should restore to the previous state and repeat the same method to randomly move the polymer. Moreover, even if the move satisfies the constraints, the different energy change causes different possibility of successful move. In the process of simulation, we notice that the translocation process is slow enough to consider as equilibrium state within every move. What's more, since the process is completely random, there's possibility that the polymer move back to *cis* space, and in this scenario, we have to restart the entire process by constructing a brand-new conformation.

In conclusion, list the entire simulation process step by step:

- (i) Construct a space divided by an invincible wall at $x=0$ with a pore on it, and the space $x < 0$ is defined as *cis* space, meanwhile, the space $x > 0$ is defined as *trans* space;
- (ii) Randomly construct a polymer chain with $N+1$ monomers in *cis* space whose first monomer is fixed at the closed pore, and the polymer satisfies the constraints under equilibrium state;
- (iii) Let the polymer chain moves for certain amount of time to equilibrium state in order to avoid the polymer maintaining contracted state which perhaps dramatically increase the required translocation time and waste computation resources;
- (iv) The pore is now open and the time is set at $t = 0$;
- (v) Randomly choose a monomer i from $N+1$ total monomers and its position

is recorded as (x_i, y_i, z_i) ;

(vi) Trial move: randomly move the monomer by dx , dy , dz in each direction which results in a new monomer position $(x_i + dx, y_i + dy, z_i + dz)$ and examine whether this trial move is allowed by constraints. If not, the system should restore to before-trial-move state and simulation return to step (v);

(vii) Calculate the polymer chain energy change ΔE caused by the trial move;


(viii) Generate a uniformly-distributed random number r between $[0, 1)$, and determine whether condition $r \leq \min[1, \exp(-\Delta E/kT)]$ is satisfied. If not, the system should restore to before-trial-move state and simulation return to step (v);

(ix) Once the last monomer has threaded through the pore, the simulation stops and record the actual translocation time τ (failed trial move excluded), the failed trial move time τ_1 . (Which means, the total simulation time should be $\tau_2 = \tau + \tau_1$).

Additionally, there are cases that during the translocation process, the first monomer moves back to *cis* space. In those situations, previous moves in this particular translocation process should be deleted and restart by constructing a new polymer chain. If one record numbers of all those failed trials, one significant quantity, translocation possibility is obtained once successful translocation appears. And the relationship between translocation possibility and external field can be studied.

It's obvious that due to the randomness of Mento Carlo simulation, single translocation process can't provide accurate statistical information, thus enormous amount of translocation process should be calculated (in the simulation, we calculate 1000 successful translocation process to determine the average translocation time).

References

- [1] J. J. Kasianowicz, E. Brandin, D. Branton, and D. W. Deamer, "Characterization of individual polynucleotide molecules using a membrane channel," *Proceedings of the National Academy of Sciences*, ~~vol. 93, no. 24, pp. 13 770–13 773, 1996~~ 
- [2] C. G. Baumann, S. B. Smith, V. A. Bloomfield, and C. Bustamante, "Ionic effects on the elasticity of single dna molecules," *Proceedings of the National Academy of Sciences*, ~~vol. 94, no. 12, pp. 6185–6190, 1997~~

- [3] M. Bulacu and E. van der Giessen, “Effect of bending and torsion rigidity on self-diffusion in polymer melts: A molecular-dynamics study,” *The Journal of chemical physics*, vol. 123, no. 11, p. 114901, 2005.
- [4] H.-P. Hsu and K. Kremer, “Static and dynamic properties of large polymer melts in equilibrium,” *The Journal of chemical physics*, vol. 144, no. 15, p. 154907, 2016.
- [5] A. Milchev, “Single-polymer dynamics under constraints: Scaling theory and computer experiment,” *Journal of Physics: Condensed Matter*, vol. 23, no. 10, p. 103101, 2011.
- [6] F. Wu, X. Yang, and M.-B. Luo, “Theoretical study on the translocation of partially charged polymers through nanopore,” *Journal of Polymer Science Part B: Polymer Physics*, vol. 55, no. 13, pp. 1017–1025, 2017.
- [7] S. Mirigian, Y. Wang, and M. Muthukumar, “Translocation of a heterogeneous polymer,” *The Journal of chemical physics*, vol. 137, no. 6, p. 064904, 2012.
- [8] J. Sarabadani, T. Ikonen, H. Mökkönen, T. Ala-Nissila, S. Carson, and M. Wanunu, “Driven translocation of a semi-flexible polymer through a nanopore,” *Scientific reports*, vol. 7, no. 1, p. 7423, 2017.
- [9] C. Wang, Y.-C. Chen, S. Zhang, and M.-B. Luo, “Translocation of diblock copolymer through compound channels: A monte carlo simulation study,” *Macromolecules*, vol. 47, no. 20, pp. 7215–7220, 2014.
- [10] S. Geggier and A. Vologodskii, “Sequence dependence of dna bending rigidity,” *Proceedings of the National Academy of Sciences*, vol. 107, no. 35, pp. 15 421–15 426, 2010.
- [11] A.-b. Li, Y.-g. Yao, and H. Xu, “Stiffness and excluded volume effects on conformation and dynamics of polymers: A simulation study,” *Chinese Journal of Polymer Science*, vol. 30, no. 3, pp. 350–358, 2012.